

# Integrated high-throughput analysis identifies Sp1 as a crucial determinant of p53-mediated apoptosis

H Li<sup>1</sup>, Y Zhang<sup>2</sup>, A Ströse<sup>3</sup>, D Tedesco<sup>4</sup>, K Gurova<sup>3</sup> and G Selivanova<sup>\*1</sup>

The restoration of p53 tumor suppressor function is a promising therapeutic strategy to combat cancer. However, the biological outcomes of p53 activation, ranging from the promotion of growth arrest to the induction of cell death, are hard to predict, which limits the clinical application of p53-based therapies. In the present study, we performed an integrated analysis of genome-wide short hairpin RNA screen and gene expression data and uncovered a previously unrecognized role of Sp1 as a central modulator of the transcriptional response induced by p53 that leads to robust induction of apoptosis. Sp1 is indispensable for the pro-apoptotic transcriptional repression by p53, but not for the induction of pro-apoptotic genes. Furthermore, the p53-dependent pro-apoptotic transcriptional repression required the co-binding of Sp1 to p53 target genes. Our results also highlight that Sp1 shares with p53 a common regulator, MDM2, which targets Sp1 for proteasomal degradation. This uncovers a new mechanism of the tight control of apoptosis in cells. Our study advances the understanding of the molecular basis of p53-mediated apoptosis and implicates Sp1 as one of its key modulators. We found that small molecules reactivating p53 can differentially modulate Sp1, thus providing insights into how to manipulate p53 response in a controlled way.

*Cell Death and Differentiation* (2014) 21, 1493–1502; doi:10.1038/cdd.2014.69; published online 27 June 2014

The malfunction of the p53 tumor suppressor pathway is required for the development of most cancers.<sup>1</sup> Reinstatement of p53 *in vivo* exerts an efficient suppression of different types of established tumors,<sup>2–4</sup> supporting the idea of pharmacological restoration of p53 to combat cancer. A set of p53-reactivating compounds, including PRIMA-1<sup>MET</sup>/Apr-246, nutlin, RITA, M1 compounds, tenovins and others, have been identified and some of them are currently being tested in clinical trials.<sup>1</sup> However, the consequences of p53 activation vary, ranging from cell death to cell survival, and are difficult to predict. As the induction of apoptosis, but not growth arrest, is the preferable outcome of pharmacological activation of p53, it is imperative to understand the mechanism of p53-mediated cell fate decisions for the efficient clinical application of p53-targeting drugs.

It is well established that the induction of pro-apoptotic genes (that is, Puma, Noxa etc) is required for the initiation of apoptosis by p53.<sup>5,6</sup> However, p53 activated by the MDM2 inhibitor nutlin, in spite of the induction of pro-apoptotic Puma and Noxa, induces cell cycle arrest in a number of cancer lines, with no signs of apoptosis.<sup>7,8</sup> Hence, the induction of pro-apoptotic genes by p53 is necessary, but not sufficient to induce efficient cell death. Several other mechanisms have been reported to contribute to p53-mediated apoptosis, including the inhibition of survival factors,<sup>8</sup> the repression of pro-survival pathways, such as Akt-PI3K<sup>8</sup> and IGFR,<sup>9</sup> and the inhibition of glycolytic enzymes.<sup>10,11</sup> But how p53 orchestrates

these distinct sets of genes to induce apoptosis remains unclear. Our previous analysis of genome-wide chromatin occupancy by p53 revealed a similar binding pattern of p53 upon nutlin, RITA and 5-fluorouracil (5-FU) treatment, regardless of the differences in transcriptional program and biological outcome.<sup>12</sup> This finding implies the importance of cofactors in p53-mediated cell fate decisions. For example, Sp1, a ubiquitous transcription factor (TF), has been shown to cooperate with p53.<sup>12–15</sup>

Recent development of the genome-wide loss-of-function screen using pooled siRNA or short hairpin RNA (shRNA) libraries facilitates the understanding of p53-mediated cell cycle arrest.<sup>7,16,17</sup> In the present study, using genome-wide shRNA screen integrated with transcriptomic and chromatin immunoprecipitation followed by deep sequencing (ChIP-seq) analysis, we addressed the mechanisms of p53-induced apoptosis in human cancer cells and identified Sp1 as one of its essential determinants.

## Results

**Genome-wide shRNA screen indicates Sp1 as a central modulator of p53-mediated apoptosis.** We tested the biological effect of five well-studied p53-activating chemical compounds, nutlin, RITA, actinomycin D (ActD), cisplatin (CDDP) and 5-FU, in three wild-type p53-expressing human cancer cell lines of different origin, including MCF-7 breast

<sup>1</sup>Department of Microbiology, Tumor and Cell Biology (MTC), Karolinska Institutet, 17177 Stockholm, Sweden; <sup>2</sup>College of Life Science, Northeast Agricultural University, Mucai Street 59, Harbin 150030, PR China; <sup>3</sup>Department of Cell Stress Biology, Roswell Park Cancer Institute, Elm and Carlton Streets, Buffalo, NY 14263, USA and <sup>4</sup>Cellecta, Inc., 320 Logue Avenue, Mountain View, CA 94043, USA

\*Corresponding author: G Selivanova, Department of Microbiology, Tumor and Cell Biology (MTC), Karolinska Institutet, Nobels vag 16, Box 280, Stockholm 17177, Sweden. Tel: +46 8 52486302 or 46 8 52486311; Fax: +46 8 342651; E-mail: Galina.Selivanova@ki.se

**Abbreviations:** ActD, actinomycin D; CDDP, cisplatin; PFT- $\alpha$ , pifithrin- $\alpha$ ; PFT- $\mu$ , pifithrin- $\mu$ ; shRNA, short hairpin RNA; SLNs, synthetic lethal nodes; RNs, resistance nodes; ChIP-seq, chromatin immunoprecipitation followed by deep sequencing; TF, transcription factor; MEFs, mouse embryonic fibroblasts; FACS, fluorescence-activated cell sorting; PI, propidium iodide; Rho123, rhodamine 123

Received 16.12.13; revised 28.3.14; accepted 23.4.14; Edited by KH Vousden; published online 27.6.14

carcinoma cells, SJSA osteosarcoma cells and HCT116 colorectal cancer cells, and an isogenic derivative of HCT116 cells with p53 deletion (HCT116 *TP53*<sup>-/-</sup> cells), as shown in Supplementary Figures S1A and B. In MCF-7 and HCT116 cells, RITA induced apoptosis (Figures 1a and b), with no signs of cell cycle arrest (Figure 1c). p53-dependence of apoptosis was confirmed by using HCT116 *TP53*<sup>-/-</sup> cells (Figure 1a). Furthermore, p53-mediated apoptosis induced by RITA was transcription-dependent, because it was totally halted by pifithrin (PFT)- $\alpha$ , a chemical inhibitor of the p53 transcriptional activity,<sup>18</sup> but not affected by PFT- $\mu$ , which inhibits p53 binding to mitochondria by reducing its affinity to anti-apoptotic proteins Bcl-xL and Bcl-2 but has no effect on p53-dependent transactivation<sup>19</sup> (Figure 1b). Therefore, we have chosen MCF-7 and HCT116 cells treated with RITA to investigate the cofactors needed for p53-mediated apoptosis. Nutlin, which predominantly induced cell cycle arrest in MCF-7 and HCT116 cells, was selected for comparison.

Next, we performed genome-wide shRNA screen in MCF-7 cells treated with RITA using a pool of lentiviral shRNA constructs, composed of 27290 shRNAs targeting 5046 known human genes (Figure 1d, see Supplementary Information Methods for details). By deep sequencing, we obtained 20 million individual measurements of the abundance of shRNAs after treatment with RITA, which reflect the effect of shRNA on apoptosis induced by RITA (Supplementary Table S1). We identified 8753 shRNAs whose abundance was significantly different in control (DMSO) and RITA-treated cells based on following criteria: (i)  $P$ -value < 0.1, (ii) FDR < 0.3 and (iii)  $P$ -values of the weighted  $Z$ -scores,  $P(wZ)$  < 0.1, which integrate the information from multiple shRNAs targeting a single gene, thus minimizing the impact of possible off-target effects. Fifteen out of these genes were selected for validation. We created cell lines stably expressing independent shRNAs (obtained from Sigma, St. Louis, MO, USA) against these genes and determined their viability after RITA treatment relative to a control cell line expressing a nontargeting shRNA (Supplementary Table S2). Validation studies showed that the depletion of 9 of 15 candidate genes changed cell viability on RITA treatment (Supplementary Table S2). Thus, our screening approach successfully identified new genes that modulate apoptosis induced by p53. To decrease the false positives, we selected a more stringent cutoff based on criteria (i)  $P$ -value < 0.05, (ii) FDR < 0.1 and (iii)  $P(wZ)$  < 0.1 for further analysis and identified 520 shRNAs. Hierarchical clustering analysis demonstrated the efficient clustering of the biological replicates of control and RITA-treated cells and revealed two groups of genes: synthetic lethal nodes (SLNs), depletion of which sensitized cells to RITA treatment (the ratio of read counts between DMSO and RITA > 1), and resistance nodes (RNs), depletion of which rendered cells resistant to RITA treatment (the ratio of read counts between DMSO and RITA < 1). Our screen for factors modulating p53-induced apoptosis revealed much less RNs than SLNs (40 RNs, 0.8% of total number of genes tested *versus* 445 SLNs, 8.03% of total number of genes) (Figure 1e). This observation is different from previous genome-wide shRNA screen<sup>8</sup> studying p53-mediated cell cycle arrest, which identified a similar number of SLNs and RNs (Supplementary Figure S2).

First, we focused our efforts on the RNs, whose depletion results in bypass of p53-mediated apoptosis. We did not identify pro-apoptotic genes (selected according to KEGG: hsa04210) among RNs (Supplementary Table S3). This suggests that the depletion of a single pro-apoptotic gene has little effect on p53-mediated apoptosis. Pathway analysis using DAVID tool could not identify any known pathway overrepresented among RNs. Therefore, we performed the analysis of functional connections between proteins encoded by RNs using STRING software. Twenty-two out of 40 RNs had at least two connections, as shown in Figure 1f. Notably, these 22 RNs were all directly or indirectly connected with Sp1. Among them, nine genes have been identified as direct transcriptional targets of Sp1, including *AKR1C1*, *TBXAS1*, *SULT1A1*, *HDP*, *SCAP*, *Sp3*, *FCER1A*, *CITED2* and *Sp1* itself (Supplementary Table S4). In addition, TAF1-mediated histone acetylation has been shown to be required for the binding of Sp1 to *cyclin D1* promoter.<sup>20</sup> Similar analysis performed with all SLNs and RNs resulted in p53 being at the center of the network together with several TFs including Sp1, AP1, SAMD2 and RXRA (Supplementary Figure S3). Among these TFs, only Sp1 was identified as RN by genome-wide shRNA screen (Supplementary Table S3). Thus, our analysis indicates that Sp1 may serve as a crucial modulator of p53-mediated apoptosis.

**Sp1 is a key determinant of p53-mediated apoptosis but is not required for p53-mediated cell cycle arrest.** Next, we addressed the effects of Sp1 on p53-induced apoptosis. Sp1 depletion resulted in a greater than 50% reduction of the apoptosis induced by RITA (Figure 2a), which was also evident in a long-term viability assay (Supplementary Figures S4A and B). Furthermore, p53-induced apoptosis upon CDDP or 5-FU treatment was rescued by Sp1 depletion as well, which excluded the possibility of a compound-specific effect (Figure 2a). Nutlin and ActD, which induced p53-mediated cell cycle arrest in MCF-7 cells, did not initiate apoptosis after Sp1 depletion (Figure 2a). However, Sp1 overexpression converted growth arrest into robust apoptosis in nutlin-treated MCF-7 and HCT116 cells (Figure 2b, Supplementary Figure S4C). This outcome was p53 dependent, as no apoptosis was induced by nutlin in p53-null cells on Sp1 overexpression (Figure 2b, Supplementary Figure S4C).

Considering the previously reported role of Sp1 in cell cycle control,<sup>21</sup> we examined the effect of Sp1 depletion on cell cycle in MCF-7 and HCT116 cells treated with RITA or nutlin. Although Sp1 depletion itself slightly increased G1 population in MCF-7, it did not change the cell cycle distribution upon RITA treatment (Figure 2c). In line with these data, an equivalent level of cell cycle arrest was induced by nutlin in Sp1-depleted and -nondepleted cells (Figure 2d), suggesting that Sp1 is not required for p53 to induce cell cycle arrest.

**Integrated analysis suggests Sp1 involvement in p53-mediated transcriptional repression.** As the apoptosis induced by p53 activation is transcription-dependent in our system, we performed the genome-wide analysis of gene expression profiles to investigate the effect of Sp1 on p53-mediated transcriptional program. Sp1 depletion significantly affected the p53 transcriptional response induced by

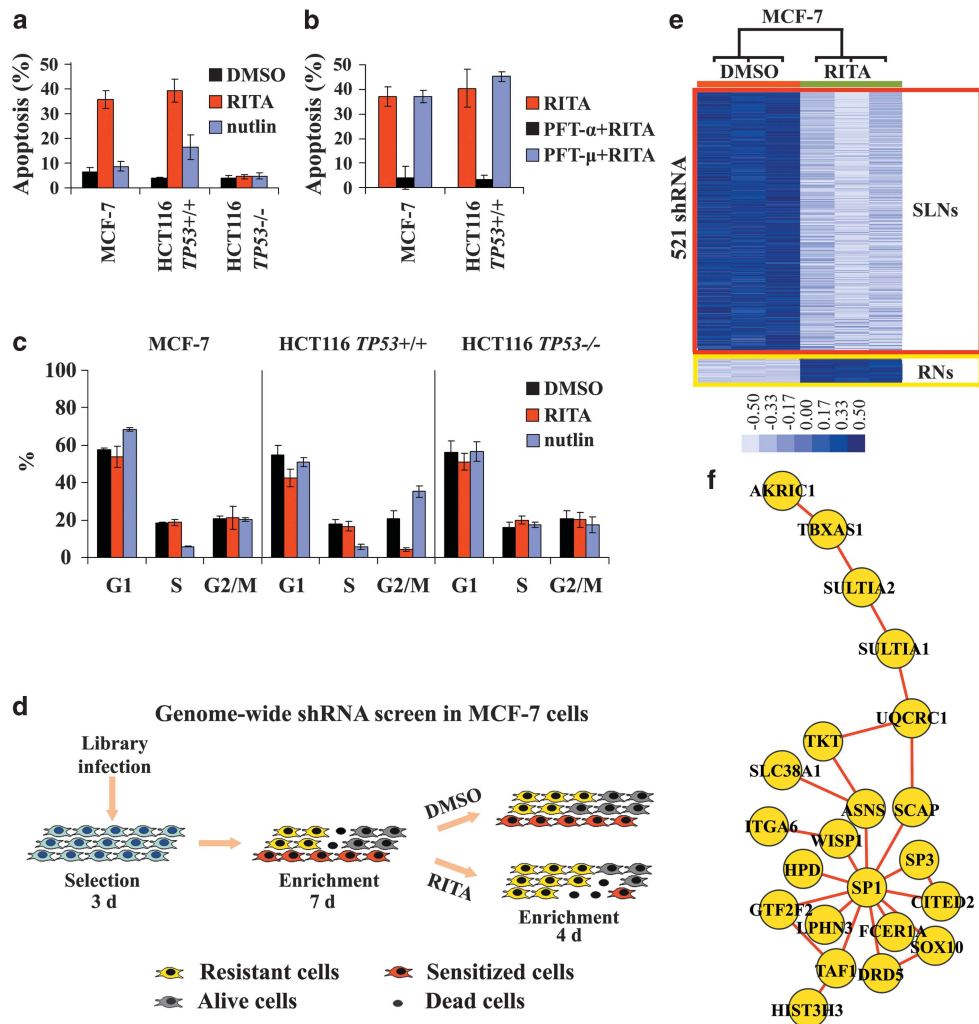


**Figure 1** Genome-wide shRNA screen for identifying modulators of p53-mediated apoptosis. (a and b) Induction of apoptosis by RITA or nutlin in MCF-7, HCT116 and HCT116 *TP53*<sup>-/-</sup> cells, as assessed by FACS of Rho123-PI-stained cells. Apoptosis was assayed also by FACS of Annexin V-PI-stained cells or sub-G1 population detection using PI staining. In each experiment, at least two methods were used, and conclusions were only made when similar results had been obtained with both methods. Detailed results are shown in Supplementary Figure S1B. (b) Induction of apoptosis by RITA was halted by blocking the p53 transcriptional activity with PFT- $\alpha$ ,<sup>18</sup> but not by blocking the cytoplasmic function of p53 with PFT- $\mu$ .<sup>19</sup> (c) Effect of RITA and nutlin on cell cycle in MCF-7, HCT116 and HCT116 *TP53*<sup>-/-</sup> cells was assessed by FACS using PI staining. (d) Schematic representation showing the design of the genome-wide shRNA screen in MCF-7 cells. (e) Hierarchical clustering analysis of the shRNA screen data identifies two groups of hits: SLNs and RNs. Light blue indicates low abundance of shRNA (SLNs) and dark blue reflects high abundance (RNs). Rows indicate shRNAs. Raw data were normalized within each shRNA.  $P < 0.05$ , FDR  $< 0.1$  and  $P(wZ) < 0.1$ . (f) Analysis of functional interactions between the RNs reveals Sp1 as a central modulator of p53-mediated apoptosis. In b, c and d, data are presented as mean  $\pm$  S.D.,  $n = 3$

RITA (Figure 3a and Supplementary Figure S5): 57.53% of induced genes and 41.91% of repressed genes were not differentially expressed in the absence of Sp1. Moreover, 37.31% of induced genes were repressed and 48.42% of repressed genes were induced in RITA-treated cells on Sp1 depletion (Figure 3b). Interestingly, the induction upon RITA treatment of some well-known p53 pro-apoptotic targets such as Noxa (*PMAIP1*), Puma (*BBC3*), Fas, *Tp53l3*, BAX, *TNFRSF10A* and *TNFRSF10B* was not reversed by Sp1 depletion (Figure 3a). Our combined analysis of shRNA screen data and microarray data showed that, when taken individually, none of these pro-apoptotic genes was absolutely required for the induction of apoptosis (Supplementary Figure S6). Actually, the expression of these pro-apoptotic p53 targets was activated both by RITA (triggering apoptosis) and nutlin

(inducing cell cycle arrest) (Figure 3a), although the expression profile induced by p53 on RITA treatment was quite different from that induced by p53 on nutlin, regardless of Sp1 status (Supplementary Figures S7A and B). These results provided a further evidence for the minor role of these pro-apoptotic genes in the rescue of cells from p53-induced apoptosis on Sp1 depletion.

In addition, genes important for cell cycle arrest, *GADD45a*, *CDKN1A*, *SESN1* and *BTG2*, were also induced by both nutlin and RITA. Moreover, the expression of these genes was still activated by RITA in Sp1-depleted cells (Supplementary Figure S7C). Thus, the induction of this set of growth arrest genes was not sufficient to induce cell cycle arrest upon RITA treatment, most probably due to the MDM2-mediated degradation of p21 and hnRNP K, as we have reported.<sup>22</sup>

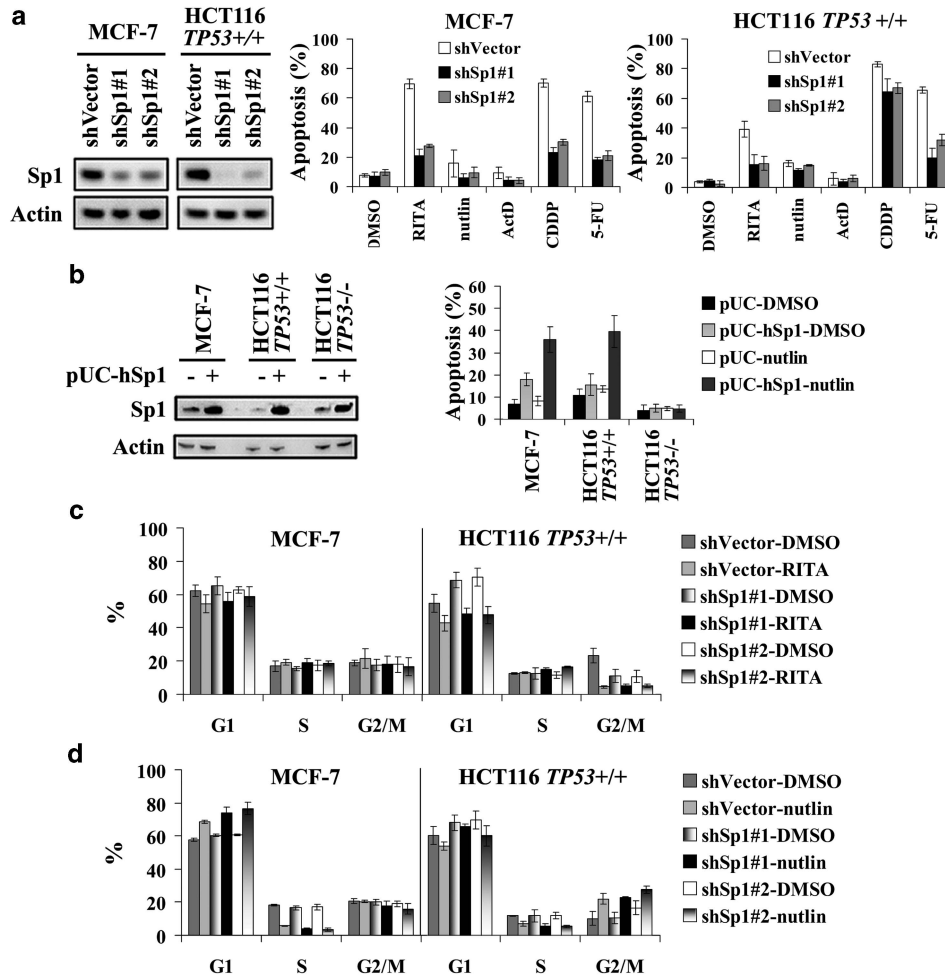


**Figure 2** Sp1 is a key determinant of p53-mediated apoptosis, but not cell cycle arrest. (a) Left panel, the depletion of Sp1 in MCF-7 and HCT116 cells with two shRNAs targeting different sequences of Sp1 was assessed by immunoblotting. Actin was used as loading control. The depletion of Sp1 reduces apoptosis induced by p53-activating compounds after 48 h in MCF-7 (middle panel) and HCT116 (right panel) cells as assessed by FACS performed as in Figure 1a. (b) Right panel, ectopic expression of Sp1 promotes apoptosis induced by nutlin in MCF-7 and HCT116 cells but not in HCT116 *TP53*<sup>-/-</sup> cells as assessed by FACS performed as in Figure 1a. Left panel, the efficiency of ectopic expression of Sp1 was assessed by immunoblotting. (c and d) Cell cycle distribution was not affected by Sp1 depletion in MCF-7 and HCT116 cells exposed to RITA (c) or nutlin (d) as assessed by FACS performed as in Figure 1c. FACS data are presented as mean ± S.D., *n* = 3

Although we did not find a pathway enriched within RNs (Figure 3c), there were 18 pathways enriched within SLNs (Supplementary Figure S8). This implies that the inhibition of certain genes from these pathways will be synthetic lethal with RITA. Besides ‘cell cycle’ and ‘apoptosis’, there are several pathways also related to apoptosis, such as ‘Wnt signaling’, ‘TGF $\beta$  signaling’, ‘MAPK signaling’, ‘Cell adhesion’ and pathways involved in metabolism.<sup>11,23–26</sup>

Pathway analysis of the microarray data revealed that 6 of these 18 synthetic lethal pathways were uniquely enriched with p53-downregulated genes upon RITA treatment, but not with p53-upregulated genes or genes altered by nutlin (Figure 3c). These data indicate the importance of p53-mediated transcriptional repression of genes involved in six pathways for the induction of apoptosis. Importantly, these six pathways were regulated in a Sp1-dependent manner, as evidenced from the analysis of microarray data in Sp1-depleted cells (Figure 3c).

In our previous study, we have demonstrated that the transcriptional repression of survival genes by p53 is required

for robust apoptosis, but we have not identified cofactors required for it.<sup>8</sup> Our results presented above suggest Sp1 as an important cofactor conferring the pro-apoptotic transcriptional repression by p53.

**Sp1 cooperation at p53 target genes is required for the p53-mediated pro-apoptotic transcriptional repression.**

To address the mechanism of co-regulation of repressed genes by p53 and Sp1, we analyzed the p53 genome occupancy on the 1078 genes, which were co-repressed by p53 and Sp1 upon RITA but not nutlin treatment (Figure 4a), using the p53 ChIP-seq data previously reported by us.<sup>12</sup> Among these genes, 227 genes were bound by p53 after RITA treatment (Figure 4b) and were enriched in 10 pathways (Supplementary Figure S9). Thus, these genes and pathways are under the direct transcriptional control of p53. Three out of these 10 pathways, ‘pathways in cancer’, ‘Wnt signaling pathway’ and ‘TGF- $\beta$  signaling pathway’, were identified as being synthetic lethal with p53-mediated apoptosis (compare Figures 3c and 4d). The other 851 genes



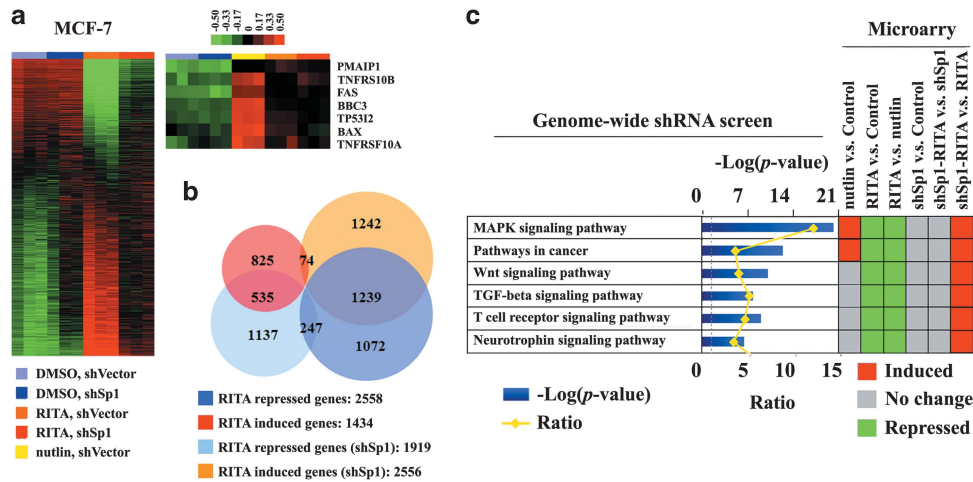


**Figure 3** Sp1 is indispensable for the pro-apoptotic transcriptional repression by p53. (a) Heatmap representation of the genome-wide gene expression profiles (left panel) and the expression profiles of pro-apoptotic genes (right panel) in MCF-7 cells with or without Sp1 depletion on RITA or nutlin treatment. Columns indicate arrays and rows indicate genes. (b) Venn diagram shows the intersection of genes significantly changed by RITA treatment in MCF-7 cells with or without Sp1 depletion.  $P < 0.001$ . (c) Combination of pathways identified via shRNA screen data and via analysis of microarray data. Pathways enriched with SLNs are presented in the left part of the panel. The overlap of pathways identified via analysis of the genome-wide shRNA screen data and the microarray data (MCF-7 cells treated with RITA or nutlin and Sp1-depleted MCF-7 cells treated with RITA) is shown in the right part of the panel. Red indicates the pathways enriched with induced genes; green indicates the pathways enriched with repressed genes.  $P < 0.05$

that were not bound by p53 are most likely repressed in an indirect way. Among the 227 p53-bound genes, 173 genes were also bound by p53 after nutlin treatment, leaving 54 unique targets for p53 activated by RITA (Figure 4b).

Using oPOSSUM, we performed motif analysis to find Sp1 response elements (RE) in p53-bound genes. Forty-eight of the 54 'RITA-unique' p53 targets and 162 of the 173 p53 targets 'common for RITA and nutlin' have been found to contain conserved Sp1 RE, thus identifying them as potential common target genes of p53 and Sp1 (Supplementary Tables S5 and S6). Interestingly, further investigation of ChIP-seq data showed that around 71% of these potential common targets contained p53-binding sites in the vicinity ( $\pm 500$  bp) of the putative Sp1 RE (Figure 4c). Analysis of functional protein association among these 227 p53 targets produced a network centered by p53 and Sp1 and including *MAPK8*, *RARA*, *SAMD3*, *CREBBP*, *RUNX1*, *BTRC* and *NCOA3* (Supplementary Figure S10).

Next, we randomly selected three genes, *DSP*, *KIAA0513* and *LARP1*, from the 54 'RITA-unique' targets, and three genes, *MAPK8*, *ARNT2* and *RARA*, from the 173 'common RITA/nutlin' targets. For each gene, we detected the binding levels of p53 and Sp1 by ChIP-PCR, using the same primers. The binding profile of p53 and the location of amplified region are shown in Supplementary Figure S11. Regardless of stimuli, p53 was bound to 'RITA-unique' genes as well as to 'common RITA/nutlin' genes tested (Figure 4e). This is consistent with our previous study showing that the majority of p53-bound sites are similar on RITA and nutlin treatment.<sup>12</sup> In line with the predicted overlap of p53-bound sites and Sp1 RE, the binding of Sp1 to all genes was significantly increased after RITA treatment (Figure 4f), suggesting a recruitment of Sp1 upon p53 activation. Furthermore, the presence of p53 at these genes was significantly reduced in Sp1-depleted cells on RITA treatment (Figure 4e). In contrast, the binding of Sp1 to these genes was not increased after nutlin treatment and

became even lower than control at *RARA* first intron (Figure 4f), indicating that p53 activated by nutlin does not recruit Sp1 to its binding sites.

We assayed the expression of selected genes by qPCR. p53 repressed these genes on RITA, but not on nutlin treatment, in spite of being present at these genes in both cases (Figure 4g). p53-mediated repression required Sp1, because the suppression of all genes tested was halted by Sp1 depletion (Figure 4g). These results confirmed the data obtained using microarray analysis.

Notably, on nutlin treatment, ectopic expression of Sp1 promoted the binding of Sp1 to *MAPK8*, *ARNT2*, *RAR*, *DSP*, *KIAA0513* and *LARP1* and repressed their transcription (Supplementary Figure S12), indicating that Sp1 overexpression may facilitate apoptosis in nutlin-treated cells via similar mechanism as that used by RITA.

Taken together, our results demonstrate that the binding of Sp1 to p53 target genes is required for the pro-apoptotic transcriptional repression by p53.

**Nutlin induces MDM2-mediated degradation of Sp1.** In line with the different binding of Sp1 to p53-repressed targets in cells treated with RITA and nutlin, we found that the protein level of Sp1 was downregulated by nutlin, but not by RITA in both MCF-7 and HCT116 cells (Figure 5a). The same results were obtained in HCT116 p53-null cells, indicating that the reduction in Sp1 protein level by nutlin was not p53 dependent (Figure 5a).

As the transcription of Sp1 was not affected by nutlin (Figure 5b), we studied the downregulation of Sp1 on posttranscription level. The half-life of the Sp1 protein was decreased by nutlin (Figure 5c). This effect was rescued via pretreatment with a proteasome inhibitor MG132 (Figure 5e), indicating proteasome-dependent degradation of Sp1. Despite the suppression of Sp1 transcription (Figure 5b), the stability of Sp1 protein was increased by RITA treatment

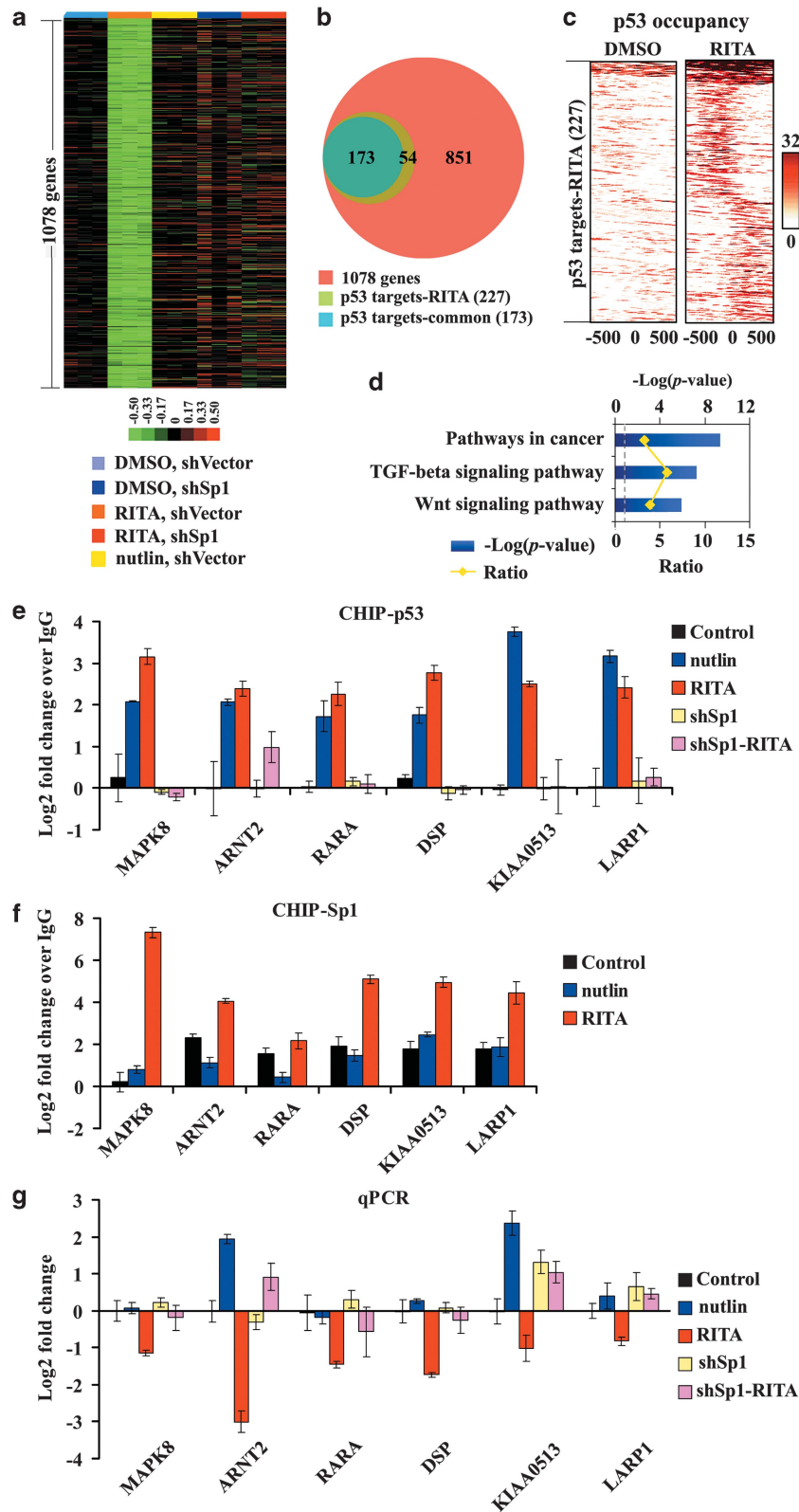


**Figure 4** p53-mediated pro-apoptotic transcriptional repression requires the co-binding of Sp1 to p53 target genes. (a) Heatmap representation of the 1078 genes whose repression by RITA was lost in Sp1-depleted cells. (b) Proportion of p53-bound genes (p53 targets) among these 1078 genes is illustrated via Venn diagram. (c) Heatmap shows p53 occupancy within  $\pm 500$  bp of the putative Sp1 RE in 227 p53-bound genes. '0' indicates the position of the putative Sp1 RE, rows indicate p53 binding (red: high peaks/binding; white: no peaks/binding). (d) Synthetic lethal pathways enriched with 227 p53-bound genes after RITA treatment.  $P < 0.05$ . (e and f) Binding of p53 (e) and Sp1 (f) to selected genes was assessed by ChIP-PCR. (g) The transcriptional level of selected genes was examined by qPCR. In e, f and g, data are presented as mean  $\pm$  S.D.,  $n = 3$

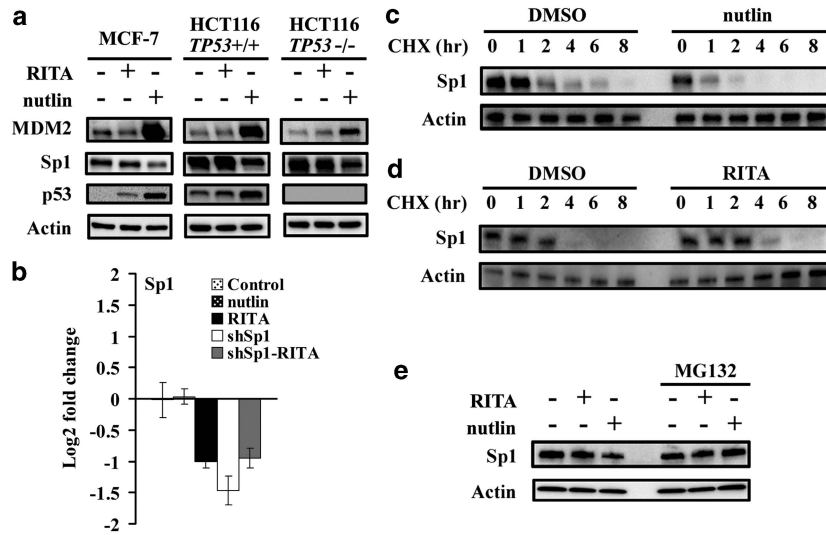


**Figure 5** Nutlin decreases Sp1 protein stability in p53-independent manner. (a) Protein levels of MDM2, Sp1 and p53 in MCF-7, HCT116 and HCT116 *TP53*<sup>-/-</sup> cells with RITA or nutlin treatment were assessed by immunoblotting. (b) mRNA level of Sp1 in MCF-7 cells with or without Sp1 depletion on RITA or nutlin treatment was examined by qPCR. Data are presented as mean  $\pm$  S.D.,  $n = 3$ . (c and d) MCF-7 cells were pretreated with nutlin (c) or RITA (d) followed by incubation with cycloheximide (CHX). Cells were collected at indicated time points after CHX treatment. Sp1 levels at different time points were measured by immunoblotting. (e) MCF-7 cells were pretreated with proteasome inhibitor MG132 followed by RITA or nutlin treatment, and Sp1 level was assessed by immunoblotting

(Figure 5d), which most probably contributes to unaffected steady-state level of the Sp1 protein upon RITA treatment.

As shown by co-immunoprecipitation assay, nutlin, but not RITA, reduced the binding of Sp1 to p53 (Supplementary Figure S13A), which was rescued by Sp1 overexpression (Supplementary Figure S13B), suggesting that the formation of p53/Sp1 complex could be directly affected by the level of Sp1.

Along with the downregulation of Sp1 by nutlin, we detected a marked induction of the MDM2 protein, a key negative regulator of p53,<sup>27</sup> on nutlin treatment in both MCF-7 and HCT116 cells (Figure 5a). We obtained similar results in HCT116 p53-null cells (Figure 5a, right panel), which is consistent with the previous study showing that nutlin can stabilize MDM2 protein in a p53-independent manner.<sup>28</sup>

It has been shown previously that Sp1 could enhance p53 degradation by MDM2 through formation of a Sp1/p53/MDM2 triple protein complex.<sup>13</sup> Given the negative correlation between Sp1 and MDM2 protein levels after nutlin treatment, we hypothesized that, on its release from p53, MDM2 stabilized by nutlin could bind to Sp1 and mediate its degradation. A prediction from this hypothesis is that the inhibition of MDM2 would restore Sp1 level on nutlin treatment.

To address this idea, two strategies were employed. First, we compared the effect of nutlin in mouse embryonic fibroblasts (MEFs) deficient for both MDM2 and p53 with that in wild-type MEFs. In wild-type MEFs, the depletion of p53 by siRNA could not prevent the induction of MDM2 and the downregulation of Sp1 by nutlin (Figure 6a). These data further confirmed that the effects of nutlin on MDM2 and Sp1 proteins were p53 independent. In contrast, in *MDM2*<sup>-/-</sup> *TP53*<sup>-/-</sup> MEFs, the downregulation of Sp1 by nutlin was compromised, in line with our prediction (Figure 6a). Further, we depleted MDM2 using pooled siRNA in HCT116 *TP53*<sup>-/-</sup> cells, which also lead to the rescue of Sp1 level on nutlin treatment (Figure 6b). On the other hand, the

overexpression of MDM2 resulted in a decreased level of Sp1 protein in MCF-7 cells, regardless of nutlin treatment, suggesting that the effect of MDM2 on Sp1 is not stimulant dependent (Figure 6c). Finally, consistent with our hypothesis, a co-immunoprecipitation assay revealed an increased level of MDM2 bound to Sp1 after nutlin, but not RITA treatment (Figure 6d). Taken together, our data demonstrate that Sp1 downregulation is mediated by nutlin-stabilized MDM2.

Next, we addressed whether MDM2-mediated repression of Sp1 on nutlin treatment is ubiquitination-dependent using MCF-7, HCT116 and HCT116 *TP53*<sup>-/-</sup> cells with MDM2 knockdown. We found that Sp1 ubiquitination was promoted by nutlin in all three cell lines, but not in cells with MDM2 knockdown (Figure 6e). Similarly, we observed the induction of Sp1 ubiquitination by nutlin in HCT116 *TP53*<sup>-/-</sup> cells expressing ectopic HA-tagged ubiquitin and the absence of enhanced Sp1 ubiquitination in MDM2-depleted cells (Figure 6f). These results support the notion that nutlin-stabilized MDM2 suppresses Sp1 via ubiquitin-dependent degradation.

Although both nutlin and RITA induced MDM2 mRNA (Supplementary Figure S14), the protein level of MDM2 was increased by nutlin, but not by RITA (Figure 5a), in line with previously published study.<sup>29</sup> We believe that this might contribute to the observed stabilization of Sp1 protein by RITA (Figure 5d). Furthermore, Sp1 was not required for the induction of either MDM2 mRNA or protein in cells treated with RITA or nutlin (Figure 6g and Supplementary Figure S14), suggesting that MDM2 is not downstream of Sp1 in the pathway that determines the cell fate upon p53 activation.

## Discussion

The pleiotropic character of the p53 network makes it hard to predict the consequence of p53 activation. The discovery of the mechanisms governing p53-mediated biological

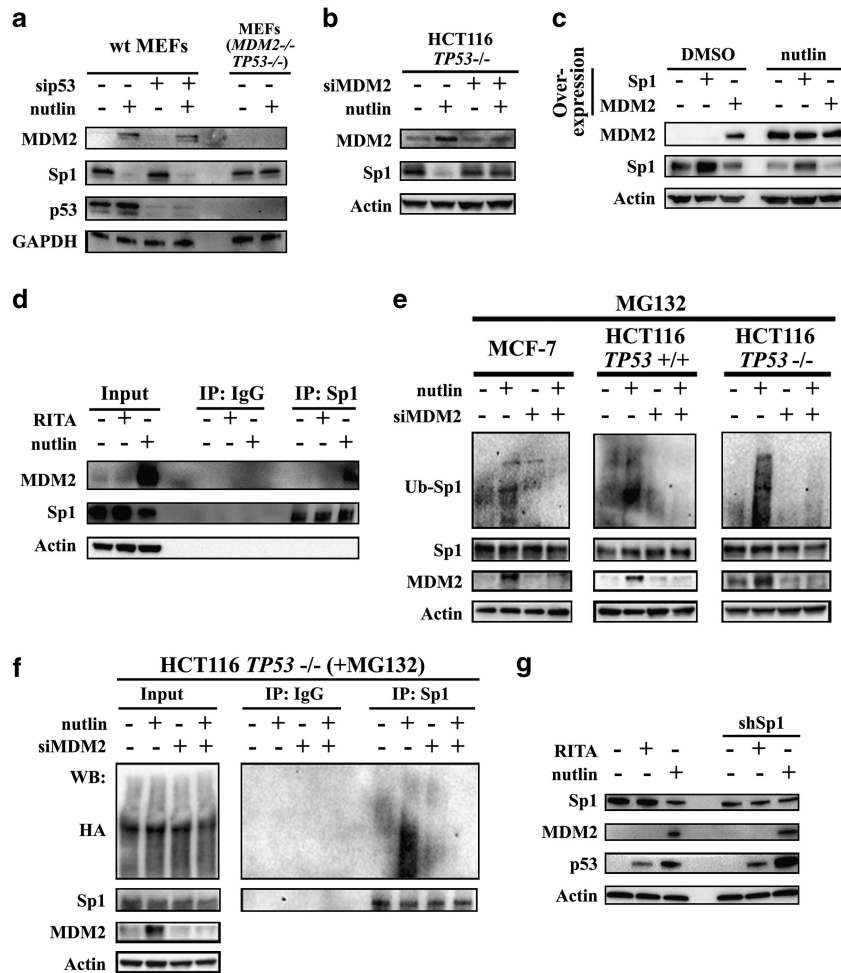


**Figure 6** MDM2 is required for the repression of Sp1 by nutlin. (a) MEFs were treated with pooled siRNA targeting p53. Protein levels of MDM2, Sp1 and p53 in wild-type MEFs and *MDM2*<sup>-/-</sup> *TP53*<sup>-/-</sup> MEFs treated with nutlin were detected by immunoblotting. GAPDH was used as loading control. (b) HCT116 p53-null cells were treated with pooled siRNA targeting MDM2. Protein levels of MDM2 and Sp1 in cells treated with nutlin were detected by immunoblotting. (c) Levels of MDM2 and Sp1 in MCF-7 cells with overexpression of Sp1 or MDM2 were assessed by immunoblotting. (d) The amount of MDM2 bound to Sp1 was detected by co-immunoprecipitation followed by immunoblotting. Right panel: equal amount of immunoprecipitated Sp1 was loaded to assess bound MDM2. (e) MCF-7, HCT116 and HCT116 *TP53*<sup>-/-</sup> cells were pretreated with pooled siRNA targeting MDM2. The level of ubiquitinated Sp1, Sp1 and MDM2 proteins was assessed in cells treated with proteasome inhibitor MG132 and nutlin by immunoblotting with anti-Sp1 and anti-MDM2 antibodies. (f) HCT116 *TP53*<sup>-/-</sup> cells expressing ectopic HA-tagged ubiquitin were pretreated with pooled siRNA targeting MDM2. The amount of HA-tagged ubiquitin attached to Sp1 was detected by the immunoprecipitation of Sp1 followed by the immunoblotting with anti-HA antibody. Actin was used as loading control. (g) Levels of MDM2, Sp1 and p53 in MCF-7 cells and Sp1-depleted MCF-7 cells on RITA or nutlin treatment were assessed by immunoblotting

outcomes is extremely important for the clinical application of p53-based therapies. Here, utilizing genome-wide shRNA screen in combination with transcriptomic and ChIP-seq analysis, we identified Sp1 as an essential determinant of p53-mediated apoptosis. We suggest the model depicted in Figure 7 showing that, upon activating stimuli, p53 induces pro-apoptotic genes encoding Puma, Noxa, Fas and others. In cells with low level of MDM2, activated p53 mediates pro-apoptotic transcriptional repression via recruitment of Sp1 to its RE in p53 target genes, which together with the induction of pro-apoptotic genes triggers efficient apoptosis. However, in cells with high level of MDM2, SP1 degradation is promoted by MDM2. Without recruitment of Sp1, p53 fails to confer pro-apoptotic transcriptional repression and, although pro-apoptotic genes are induced, efficient apoptosis is not triggered.

Although RITA treatment significantly altered the transcription of around 50% of genes in MCF-7 cells, surprisingly, no particular gene or pathway was found to be absolutely necessary for p53-mediated apoptosis. Therefore, the inactivation of a single p53-induced gene or pathway is unlikely to confer resistance in a clinical setting. In contrast, we observed a cumulative effect of RITA-repressed genes on p53-mediated apoptosis, indicating the importance of p53-mediated transcriptional repression for therapeutic effect.

The major efforts to awaken p53-mediated apoptosis in cancer cells are focused on the prevention of the binding of MDM2 to p53. However, the consequences of MDM2 inhibition vary depending on cell type. Here we show that the protection of p53 cofactor Sp1 from MDM2-mediated degradation is crucial for the efficient induction of apoptosis by



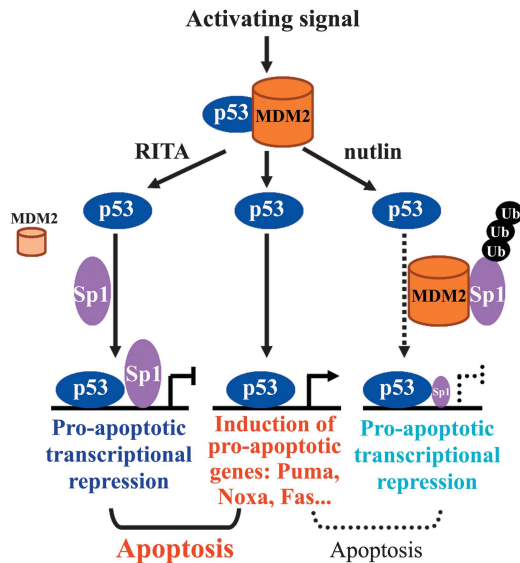


**Figure 7** Model depicting the contribution of Sp1 to p53-mediated pro-apoptotic transcriptional repression and apoptosis. See Discussion for details

p53. Our study indicates that further elucidation of MDM2 substrates involved in p53 signaling may provide new targets and help to develop more efficient strategies for p53-MDM2-based therapies.

#### Materials and Methods

**Cells, plasmid and transfections.** HCT116 and HCT116 *TPp53*<sup>-/-</sup> cells were a gift from B Vogelstein (John Hopkins University, USA). MDM2 and p53 siRNA was from Santa Cruz (Dallas, TX, USA), and GFP siRNA was from Oligoengine (Seattle, WA, USA). pUC-hSp1 and pUC-empty plasmids were gifts from Dr. D Xu (Karolinska Institute, SE). Plasmid transfections and siRNA transfections were performed using Lipofectamine 2000 (Invitrogen, Grand Island, NY, USA) according to manufacturer's instructions. All shRNAs, except the library for shRNA screen, were from Sigma, Sp1-depleted cell line was established as previously described.<sup>11</sup> All cells were grown in IMDM medium with 10% FBS (Invitrogen) as previously described<sup>28</sup> and were treated with compounds for 8 h for molecular biology assays and 3 days for fluorescence-activated cell sorting (FACS) assay, except special indication.

**Reagents.** RITA was obtained from National Cancer Institute (NCI). Nutlin, 5-FU, ActD, CDDP, PFT- $\alpha$ , PFT- $\mu$ , cycloheximide, MG132, propidium iodide (PI) and Rhodamine 123 (Rho123) were from Sigma.

**Growth suppression assays.** FACS was performed on BD FACScan. Analysis was performed using a FACScan with CellQuest software version 4.0.2 (BD, Mountain View, CA, USA). Apoptosis was assayed by FACS using Annexin V-PI staining, Sub-G1 population detection using PI staining as described in Enge *et al.*<sup>22</sup> or Rho123-PI staining as described in Ferlini *et al.*<sup>30</sup> Cell cycle and colony formation assay were detected as described in Enge *et al.*<sup>22</sup>

**Microarray analysis, ChIP-seq, qPCR and chromatin immunoprecipitation.** Expression profiling of MCF-7 cells was performed using Affymetrix (Santa Clara, CA, USA) human genome 219 arrays as previously described.<sup>11</sup> ChIP-seq data in MCF-7 cells have been reported in Nikulenkov *et al.*<sup>12</sup> Real-time qPCR and ChIP-PCR were performed as described in Li *et al.*<sup>31</sup> Primer sequences are presented in Supplementary Table S7.

**Protein extraction and western blots.** Western blots were performed according to procedures described in Zawacka-Pankau *et al.*<sup>11</sup> Following antibodies were used for western blotting: p53 (DO-1, Santa Cruz); MDM2 (2A10), Sp1 (PEP2), HA (sc-7392) and GAPDH (H-12) (all from Santa Cruz

Biotechnology); Actin (Sigma). For the ubiquitination assay, 10 mM NEM was added to the lysis buffer.

**High-throughput data analysis.** Microarray data were analyzed with R (<http://www.r-project.org/>). Pathway analysis was performed with DAVID (gene-enrichment analysis using EASE score, a modified Fisher exact *P*-value, as threshold).<sup>32</sup> ChIP-seq data were analyzed with a web-based tool, Galaxy.<sup>33</sup> Functional protein network analysis was performed with STRING.<sup>34</sup> Putative binding sites of Sp1 were predicted using oPOSSUM.<sup>35</sup>

**Genome-wide pooled shRNA screen.** Genome-wide pooled shRNA screen was performed in MCF-7 cells treated with RITA using a lentivirus-delivered pool of 27 290 shRNAs targeting 5046 known human genes. The experimental procedure and the data processing are described in Supplementary Information Materials and Methods.

**Statistics.** The SPSS software package (SPSS for Windows, Release 13.0 for Windows, SPSS Inc., Chicago, IL, USA) was used for statistical analysis. Data obtained from several experiments are reported as mean  $\pm$  S.D. Student's *t*-test was used to determine statistical significance. A *P*-value of  $<0.05$  was considered significant.

#### Conflict of Interest

The authors declare no conflict of interest.

**Acknowledgements.** This study was funded by the Swedish Cancer Society, the Swedish Research Council, Karolinska Institutet, European Commission FP6, Ragnar Söderberg foundation and the RPAF/shRNA/Collecta project funding from Roswell Park Cancer Institute. The publication reflects only the authors' views. The European Commission is not liable for any use of information herein. We are greatly indebted to our colleagues who shared valuable reagents with us, and grateful to Dr. Marcela Franco and Carsten Bahr for the technical support and valuable suggestions.

- Selivanova G. Therapeutic targeting of p53 by small molecules. *Semin Cancer Biol* 2010; **20**: 46–56.
- Martins CP, Brown-Swigart L, Evan GI. Modeling the therapeutic efficacy of p53 restoration in tumors. *Cell* 2006; **127**: 1323–1334.
- Ventura A, Kirsch DG, McLaughlin ME, Tuveson DA, Grimm J, Lintault L *et al.* Restoration of p53 function leads to tumour regression *in vivo*. *Nature* 2007; **445**: 661–665.
- Xue W, Zender L, Miething C, Dickins RA, Hernandez E, Krizhanovskiy V *et al.* Senescence and tumour clearance is triggered by p53 restoration in murine liver carcinomas. *Nature* 2007; **445**: 656–660.
- Vousden KH, Prives C. Blinded by the light: the growing complexity of p53. *Cell* 2009; **137**: 413–431.
- Valente LJ, Gray DH, Michalak EM, Pinon-Hofbauer J, Egle A, Scott CL *et al.* p53 efficiently suppresses tumor development in the complete absence of its cell cycle inhibitory and proapoptotic effectors p21, Puma, and Noxa. *Cell Rep* 2013; **3**: 1339–1345.
- Sullivan KD, Padilla-Just N, Henry RE, Porter CC, Kim J, Tentler JJ *et al.* ATM and MET kinases are synthetic lethal with nongenotoxic activation of p53. *Nat Chem Biol* 2012; **8**: 646–654.
- Grinkevich VV, Nikulenkov F, Shi Y, Enge M, Bao W, Maljukova A *et al.* Ablation of key oncogenic pathways by RITA-reactivated p53 is required for efficient apoptosis. *Cancer Cell* 2009; **15**: 441–453.
- Xiong L, Kou F, Yang Y, Wu J. A novel role for IGF-1R in p53-mediated apoptosis through translational modulation of the p53-Mdm2 feedback loop. *J Cell Biol* 2007; **178**: 995–1007.
- Bensaad K, Tsuruta A, Selak MA, Vidal MN, Nakano K, Bartrons R *et al.* TIGAR, a p53-inducible regulator of glycolysis and apoptosis. *Cell* 2006; **126**: 107–120.
- Zawacka-Pankau J, Grinkevich VV, Hüntten S, Nikulenkov F, Gluch A, Li H *et al.* Inhibition of glycolytic enzymes mediated by pharmacologically activated p53: targeting Warburg effect to fight cancer. *J Biol Chem* 2011; **286**: 41600–41615.
- Nikulenkov F, Spinnler C, Li H, Tonelli C, Shi Y, Turunen M *et al.* Insights into p53 transcriptional function via genome-wide chromatin occupancy and gene expression analysis. *Cell Death Differ* 2012; **19**: 1992–2002.
- Lin RK, Wu CY, Chang JW, Juan LJ, Hsu HS, Chen CY *et al.* Dysregulation of p53/Sp1 control leads to DNA methyltransferase-1 overexpression in lung cancer. *Cancer Res* 2010; **70**: 5807–5817.
- Bocangel D, Sengupta S, Mitra S, Bhakat KK. p53-Mediated down-regulation of the human DNA repair gene O6-methylguanine-DNA methyltransferase (MGMT) via interaction with Sp1 transcription factor. *Anticancer Res* 2009; **29**: 3741–3750.

15. Gualberto A, Baldwin AS Jr. p53 and Sp1 interact and cooperate in the tumor necrosis factor-induced transcriptional activation of the HIV-1 long terminal repeat. *J Biol Chem* 1995; **270**: 19680–19683.
16. Berns K, Hijmans EM, Mullenders J, Brummelkamp TR, Velds A, Heimerikx M *et al*. A large-scale RNAi screen in human cells identifies new components of the p53 pathway. *Nature* 2004; **428**: 431–437.
17. Brummelkamp TR, Fabius AW, Mullenders J, Madiredjo M, Velds A, Kerkhoven RM *et al*. An shRNA barcode screen provides insight into cancer cell vulnerability to MDM2 inhibitors. *Nat Chem Biol* 2006; **2**: 202–206.
18. Komarov PG, Komarova EA, Kondratov RV, Christov-Tselkov K, Coon JS, Chernov MV *et al*. A chemical inhibitor of p53 that protects mice from the side effects of cancer therapy. *Science* 1999; **285**: 1733–1737.
19. Strom E, Sathe S, Komarov PG, Chernova OB, Pavlovska I, Shyshynova I *et al*. Small-molecule inhibitor of p53 binding to mitochondria protects mice from gamma radiation. *Nat Chem Biol* 2006; **2**: 474–479.
20. Hilton TL, Li Y, Dunphy EL, Wang EH. TAF1 histone acetyltransferase activity in Sp1 activation of the cyclin D1 promoter. *Mol Cell Biol* 2005; **25**: 4321–4332.
21. Grinstein E, Jundt F, Weinert I, Wernet P, Royer HD. Sp1 as G1 cell cycle phase specific transcription factor in epithelial cells. *Oncogene* 2002; **21**: 1485–1492.
22. Enge M, Bao W, Hedström E, Jackson SP, Moumen A, Selivanova G. MDM2-dependent downregulation of p21 and hnRNP K provides a switch between apoptosis and growth arrest induced by pharmacologically activated p53. *Cancer Cell* 2009; **15**: 171–183.
23. Pečina-Slaus N. Wnt signal transduction pathway and apoptosis: a review. *Cancer Cell Int* 2010; **10**: 22.
24. Zeng L, Rowland RG, Lele SM, Kyrianiou N. Apoptosis incidence and protein expression of p53, TGF-beta receptor II, p27Kip1, and Smad4 in benign, premalignant, and malignant human prostate. *Hum Pathol* 2004; **35**: 290–297.
25. Brown L, Benchimol S. The involvement of MAPK signaling pathways in determining the cellular response to p53 activation: cell cycle arrest or apoptosis. *J Biol Chem* 2006; **281**: 3832–3840.
26. Ilić D, Almeida EA, Schlaepfer DD, Dazin P, Aizawa S, Damsky CH. Extracellular matrix survival signals transduced by focal adhesion kinase suppress p53-mediated apoptosis. *J Cell Biol* 1998; **143**: 547–560.
27. Wade M, Li YC, Wahl GM. MDM2, MDMX and p53 in oncogenesis and cancer therapy. *Nat Rev Cancer* 2013; **13**: 83–96.
28. van Leeuwen IM, Higgins M, Campbell J, Brown CJ, McCarthy AR, Pirrie L *et al*. Mechanism-specific signatures for small-molecule p53 activators. *Cell Cycle* 2012; **10**: 1590–1598.
29. Rinaldo C, Prodosmo A, Siepi F, Moncada A, Sacchi A, Selivanova G *et al*. HIPK2 regulation by MDM2 determines tumor cell response to the p53-reactivating drugs Nutlin-3 and RITA. *Cancer Res* 2009; **69**: 6241–6248.
30. Ferlini C, Scambia G. Assay for apoptosis using the mitochondrial probes, Rhodamine123 and 10-N-nonyl acridine orange. *Nat Protoc* 2007; **2**: 3111–3114.
31. Li H, Lakshminanth T, Garofalo C, Enge M, Spinnler C, Anichini A *et al*. Pharmacological activation of p53 triggers anticancer innate immune response through induction of ULBP2. *Cell Cycle* 2011; **10**: 3346–3358.
32. Blankenberg D, Von Kuster G, Coraor N, Ananda G, Lazarus R, Mangan M *et al*. Galaxy: a web-based genome analysis tool for experimentalists. *Curr Protoc Mol Biol* 2010; **Chapter 19**: Unit 19.10.1–21.
34. Franceschini A, Szklarczyk D, Frankild S, Kuhn M, Simonovic M, Roth A *et al*. STRING v9.1: protein-protein interaction networks, with increased coverage and integration. *Nucleic Acids Res* 2013; **41**(Database issue): D808–D815.
35. Ho Sui SJ, Mortimer JR, Arenillas DJ, Brumm J, Walsh CJ, Kennedy BP *et al*. oPOSSUM: identification of over-represented transcription factor binding sites in co-expressed genes. *Nucleic Acids Res* 2005; **33**: 3154–3164.



This work is licensed under a Creative Commons Attribution-NonCommercial-NoDerivs 3.0 Unported License. The images or other third party material in this article are included in the article's Creative Commons license, unless indicated otherwise in the credit line; if the material is not included under the Creative Commons license, users will need to obtain permission from the license holder to reproduce the material. To view a copy of this license, visit <http://creativecommons.org/licenses/by-nc-nd/3.0/>

Supplementary Information accompanies this paper on Cell Death and Differentiation website (<http://www.nature.com/cdd>)